

Preparation of docetaxel-loaded, glycyrrhetic acid-modified nanoparticles and their liver-targeting and antitumor activity

HANTAO XUE^{1*}, LIYA QIN^{1*}, LONGXIANG ZHANG², XIAOCHENG LI¹, FEI WU¹, WEIYU WANG¹, CHEN WANG¹, WENBIN DIAO¹, BIN JIANG¹, BO LIAN¹, JINGLIANG WU¹, JINGKUN BAI¹, TONGYI SUN¹, CHUNLING ZHAO¹, MEIHUA QU², WENJING YU¹, YUBING WANG¹ and ZHIQIN GAO¹

¹Shandong Key Laboratory of Medical and Health Sciences, Key Laboratory of Biotechnological Medicine in Universities of Shandong, School of Bioscience and Technology, Weifang Medical University;

²Department of Pharmacology, Laboratory of Applied Pharmacology, College of Pharmacy, Weifang Medical University, Weifang, Shandong 261053, P.R. China

Received December 20, 2019; Accepted June 25, 2021

DOI: 10.3892/etm.2021.10578

Abstract. Liver cancer is one of the most common malignancies worldwide and poses a serious threat to human health. The most important treatment method, liver cancer chemotherapy, is limited due to its high toxicity and poor specificity. Targeted drug delivery systems have emerged as novel therapeutic strategies that deliver precise, substantial drug doses to target sites via targeting vectors and enhance the therapeutic efficacy. In the present study, glycyrrhetic acid-modified hyaluronic acid (GA-HA) was used as a carrier for the model drug docetaxel (DTX) to prepare DTX-loaded GA-HA nanoparticles (DTX/GA-HA-NPs). The results indicated that the DTX/GA-HA-NPs exhibited high monodispersity (particle dispersity index, 0.209 ± 0.116) and desirable particle size (208.73 ± 5.0 nm) and zeta potential (-27.83 ± 3.14 mV). The drug loading capacity and encapsulation efficiency of the NPs were 12.59 ± 0.68 and $85.38 \pm 4.62\%$, respectively. Furthermore, it was determined that FITC-GA-HA was taken up by cells and distributed in the cytoplasm. DTX and DTX/GA-HA (just the DTX delivered by the nanoparticle) aggregated and altered the structure of cellular microtubules. Compared with DTX alone, DTX/GA-HA-NPs had a stronger inhibitory effect on HepG2 cell proliferation and promoted apoptosis of HepG2 cells. All experimental results indicated that DTX/GA-HA-NPs were

successfully prepared and had liver-targeting and antitumor activities *in vitro*, which provided a foundation for future *in vivo* studies of the antitumor effects of DTX/GA-HA-NPs.

Introduction

Liver cancer, which includes primary and secondary liver cancer, is one of the most common malignancies (1-3). Over the past few decades, the incidence of liver cancer has significantly increased due to a lack of effective therapeutic strategies, and the incidence and mortality of liver cancer are the fifth and third highest, respectively, of all cancers (4). Hepatocellular carcinoma (HCC), a type of primary liver cancer, has a mortality rate of 51%, making it one of the deadliest malignancies worldwide. Chemotherapy is currently the most common treatment for HCC, apart from surgical resection. However, most chemotherapy drugs have high toxicities and poor specificities to cancer cells, leading to immune system damage (5). Therefore, novel HCC treatment strategies are urgently required. Nanoparticle (NP)-based targeted drug delivery has been rapidly developed as a novel therapeutic strategy for diagnosing and treating tumors. Such NP-based systems selectively deliver chemotherapy drugs to tumor sites, increase the concentration of drugs at tumor sites and prolong drug half-lives (6). They also mitigate side effects by reducing dosages of chemotherapy drugs to achieve the same therapeutic goals. Numerous receptors mediate active liver-targeted drug delivery for the treatment of liver cancer, including the asialoglycoprotein receptor (7), glycyrrhetic acid (GA) receptor (GA-R) (8-10), hyaluronan (HA) receptor (11-13) and folate receptor (14,15).

GA is a pentacyclic triterpenoid obtained from the roots of *Glycyrrhiza glabra* L. (16). Numerous studies have indicated that GA specifically combines with the GA-R widely expressed on the surface of liver parenchymal cells. Furthermore, liver tumor tissues possess 1.5-5-fold more GA-R than adjacent normal liver tissues (17). Thus, a GA-functionalized NP system possesses strong liver cell targeting and liver distribution characteristics. HA is a natural hydrophilic acid mucopolysaccharide that consists of repeating disaccharides

Correspondence to: Professor Zhiqin Gao or Dr Yubing Wang, Shandong Key Laboratory of Medical and Health Sciences, Key Laboratory of Biotechnological Medicine in Universities of Shandong, School of Bioscience and Technology, Weifang Medical University, 7166 Baotong West Street, Weifang, Shandong 261053, P.R. China
E-mail: zhiqingao2013@163.com
E-mail: ybwang@wfmc.edu.cn

*Contributed equally

Key words: glycyrrhetic acid, hyaluronic acid, docetaxel, nanoparticles, microtubules, cytotoxicity

of D-glucuronic acid and N-acetyl-D-glucosamine and may specifically combine with CD44, which is highly expressed on certain cells, including tumor cells, dendritic cells and certain epithelial cells (18). In addition, HA has excellent biological properties, such as biological compatibility, biodegradability and low toxicity (19). Therefore, HA is an ideal carrier polymer in the construction of NPs for the targeted delivery of drugs. Numerous studies have indicated that GA-functionalized hyaluronic acid NPs selectively target liver tumor tissue and liver cancer cells and reduce adverse reactions when loaded with antitumor drugs, such as doxorubicin (DOX), paclitaxel (PTX) and 5-fluorouracil (20-22).

Docetaxel (DTX), a member of the taxane family, is a semi-synthetic analogue of PTX and a microtubule depolymerization inhibitor (23). It inhibits tumor cell proliferation and exerts its antitumor effects by preventing mitosis. DTX is a front-line, standard-of-care chemotherapeutic drug for the treatment of several cancer types, including liver, ovarian, breast (24), prostate, bladder, gastric and non-small-cell lung cancers (25,26). Furthermore, previous studies have suggested that DTX reduces hepatocellular tumor size in nude mice and inhibits the proliferation of HepG2 cells. However, DTX has various disadvantages, such as low water solubility, poor stability, hypersensitivity, hemolysis and toxic side effects (27). These disadvantages limit its application to a certain extent.

The purpose of the present study was to assemble a DTX-loaded carrier based on GA-modified HA (GA-HA) NPs (DTX/GA-HA-NPs), examine the physicochemical properties of the NP system and assess its ability to deliver DTX to HepG2 cells, a liver cancer cell line commonly used in liver cancer research. The present study lays a foundation for novel, effective HCC treatment strategies.

Materials and methods

Preparation of DTX/GA-HA NPs. GA-HA was prepared as described in the previous literature (28). In brief, GA (1.41 g) and 4-(4,6-dimethoxy-1,3,5-triazin-2-yl)-4-methylmorpholinium chloride (DMT-MM) 0.967 g were stirred in 30 ml methanol overnight at 25°C and thin layer chromatography was used to monitor the formation of the product GA-ES. After rotary evaporation, 30 ml ethylenediamine was added and the mixture was stirred overnight at 25°C to obtain the product GA-NH₂. HA (60 mg) was dissolved in 10 ml distilled water, and GA-NH₂ (28.43 mg) and an appropriate amount of absolute ethanol (~0.3-0.4 ml) were added to dissolve the components. Subsequently, DMT-MM condensing agent was added and the mixture was filled into a pre-treated dialysis bag for dialysis. After freeze-drying, a theoretical degree of substitution of 10% GA-HA NPs was obtained in the freeze-dried product.

DTX/GA-HA-NPs were prepared by an ultrasonic dispersion method in three steps. In brief, GA-HA-NPs (30 mg) were dissolved in 5 ml formamide. DTX (6 mg) (Shanghai Aladdin Bio-Chem Technology Co. Ltd.) was dissolved in 200 μ l ethyl alcohol and added dropwise to the GA-HA solution. Subsequently, the mixtures were stirred at room temperature (25°C) overnight and dialyzed against distilled water for 24 h. Finally, the DTX/GA-HA-NPs were sonicated with a probe-type ultrasonicator (working power was 5%; active

every 2 sec for a 3-sec duration) in an ice bath for 0.5 h and then lyophilized with a lyophilizer.

Preparation of FITC-labeled GA-HA-NPs. The synthesis of FITC-labeled GA-HA-NPs (FITC-GA-HA-NPs) was based on the reaction between the isothiocyanate group of FITC and the amino group of HA. FITC-GA-HA-NPs were prepared by a dialysis method. The FITC-GA-HA copolymers were synthesized via two steps. First, GA-HA-NPs (50 mg) were dissolved in 10 ml mixture buffer solution (0.1 M Na₂CO₃, 0.1 M NaHCO₃, pH 9.5). FITC (5 mg) was dissolved in 1 ml ethyl alcohol and added dropwise to the GA-HA solution. The mixtures were stirred at room temperature for 24 h. Subsequently, the FITC-GA-HA was dialyzed against distilled water for 3 days and lyophilized. All procedures were performed in the dark.

Particle size and zeta potential. The DTX/GA-HA-NPs were then characterized. The particle size distribution and zeta potential of DTX/GA-HA were determined using a Zetasizer Nano ZS 90 laser particle analyzer (Malvern Panalytical). Tests were performed three times to calculate average values.

Morphological characterization. A JEM1400 transmission electron microscope (TEM; JEOL, Ltd.) was used to observe the morphology of DTX/GA-HA-NPs. First, a drop of the DTX/GA-HA-NP suspension was placed onto a super-thin, carbon-coated copper grid. Subsequently, the grid was allowed to dry at room temperature and was dyed with phosphotungstic acid for 2 min. Finally, the grid was examined with the TEM.

Drug encapsulation efficiency (EE) and loading capacity (LC). According to the requirements of the Chinese Pharmacopoeia for the determination of DTX content, and with reference to the literature (29-31), the content of DTX in DTX/GA-HA NPs was determined by high-performance liquid chromatography (HPLC; LC-2010; Shimadzu Corporation) with UV detection at 232 nm. In brief, a standard curve of DTX at 232 nm was drawn using octadecyl silane-bonded silica gel as the filler and 0.043 mol/l ammonium acetate and acetonitrile (45:55) as the mobile phase. A known amount of freeze-dried DTX-NPs was dissolved in distilled water and diluted with methanol. The amount of DTX was measured using the optical density of the DTX/GA-HA-NPs at 232 nm. The EE and LC of DTX were calculated according to the following equations: EE (%) = (M₂/M₁) x100; and LC (%) = (M₂/M₁) x100, where M¹ is the initial weight of DTX, M₂ is the weight of DTX in NPs and M₁ is the weight of lyophilized DTX/GA-HA-NPs.

In vitro drug release study. The *in vitro* release of DTX from DTX/GA-HA was investigated using the dialysis diffusion method (32-34) in PBS (pH 7.4). In brief, 5 ml of DTX/GA-HA NPs was added to a dialysis bag (molecular weight, 3,500 Da). The dialysis bag was kept in a conical flask containing 50 ml PBS at 37±0.5°C with horizontal shaking (1.11 x g). At 0.5, 1, 2, 3, 6, 9, 12, 24 and 48 h, the release medium outside the dialysis bag was replaced with fresh PBS and the removed release medium was examined by HPLC. The concentration of the released drug was determined from the absorbance intensity of DTX at 232 nm.

Cell culture. The human liver cancer cell line HepG2 was purchased from the Chinese Typical Culture Preservation Center (School of Life Sciences, Wuhan University) and the human breast cancer cell line MCF-7 was acquired from the Experimental Center at Weifang Medical University. All cell lines were cultured using DMEM/high glucose medium (Thermo Fisher Scientific, Inc.) containing 10% fetal bovine serum (FBS; ExCell Bio) at 37°C in a cell incubator with 5% CO₂.

The human liver cancer cell line HepG2 was authenticated. An appropriate amount of HepG2 cells (1x10⁶) was used to extract DNA with Chelex100 resin (Bio-Rad Laboratories, Inc.), 21 CELLID System (Sigma-Aldrich; Merck KGaA) was used to amplify 20 short tandem repeat loci and sex identification sites, and an ABI3130x1 genetic analyzer (Applied Biosystems; Thermo Fisher Scientific, Inc.) was utilized for PCR product detection. Gene Mapper IDX software (cat. no. A39978; Applied Biosystems; Thermo Fisher Scientific, Inc.) was used to analyze the test results and compare them with database Cellosaurus (<https://web.expasy.org/cellosaurus/>).

In vitro cellular uptake. The liver-targeting ability of GA-HA-NPs was evaluated with an *in vitro* cellular uptake assay. The near-infrared fluorescent dye FITC was used as a probe and observed by confocal laser scanning microscopy (CLSM; TCS SP8; Leica Microsystems). First, HepG2 cells and MCF-7 cells harvested in the exponential growth phase were seeded in 6-well plates at a density of 2x10⁵ cells/well and incubated overnight at 37°C. Subsequently, the cells were incubated with fresh DMEM containing FITC-GA-HA-NPs for 2 h at 37°C. The cells were then washed three times with PBS and fixed with a 4% paraformaldehyde for 10 min at 25°C. Finally, the cells were counterstained with Hoechst 33342 for 15 min and observed by CLSM.

In vitro cytotoxicity assay and colony formation assay. The cytotoxicity of the DTX/GA-HA-NPs to HepG2 cells was evaluated using the Cell Counting Kit-8 (CCK-8) assay. HepG2 cells were seeded in 96-well plates (6x10³ cells/well). After incubation overnight, 100 µl of DMEM containing different concentrations of GA-HA-NPs, free DTX or DTX/GA-HA NPs (concentrations of free DTX: 1, 2, 5, 10 and 20 µg/ml) were added, followed by incubation for 24 or 48 h. Subsequently, 10 µl CCK-8 solution was added to each well and the plates were incubated for another 4 h at 37°C in a cell incubator with 5% CO₂. Finally, to quantify the live cells, the 96-well plates were read in a microplate reader (Perkin Elmer) to measure optical density at 450 nm. Untreated cells were used as controls. Cell viability was calculated according to the following equation: Cell inhibition rate (%) = [1-(A/B)] x100, where A is the optical density of cells incubated with DMEM containing different concentrations of GA-HA-NPs, free DTX or DTX/GA-HA-NPs, and B is the optical density of cells incubated with DMEM alone.

For the colony formation assay, HepG2 cells were seeded in 6-well plates (0.5x10³ cells/well) and maintained until adherent. Subsequently, 2 ml free DTX (15.00 µg/ml) or DTX/GA-HA-NPs (17.65 µg/ml) diluted with DMEM containing 10% FBS were added, followed by incubation for 24 h. Subsequently, the cells were cultured for 12 days with

DMEM containing 10% FBS until colonies were generated. Finally, the colonies were fixed with 4% paraformaldehyde for 15 min at 25°C and stained with 0.1% crystal violet solution for 30 min. The number of cell colonies for different treatments were counted using ImageJ v.1.8.0_172 (National Institutes of Health).

Cell apoptosis detection using flow cytometry and fluorescence microscopy. Treated cells were fixed with 4% paraformaldehyde for 20 min at 25°C, permeabilized with 0.2% Triton X-100 for 20 min and stained with DAPI for 10 min at 25°C. Next, images of the cells were acquired using a fluorescence microscope. Cell apoptosis was determined as previously demonstrated (35).

Microtubule cytoskeleton detection using immunofluorescence staining. Immunofluorescence staining was used to observe changes in α -tubulin. In brief, HepG2 cells were seeded on 12-mm coverslips coated with poly-lysine (1x10⁵ cells/well) in a 24-well plate. Following overnight incubation, the cells were treated with free DTX or DTX/GA-HA-NPs for 24 h. Next, the cells were fixed with 4% paraformaldehyde for 15 min and permeabilized with 0.5% Triton X-100 (Sigma-Aldrich; Merck KGaA) for 15 min at room temperature after being washed 3 times with PBS on a shaker. After blocking with 5% bovine serum albumin (Beijing Solarbio Science & Technology Co., Ltd.) in PBS at room temperature for 1 h, the cells were incubated with the Tubulin-Tracker Red antibody (1:250 dilution; cat. no. C1050; Beyotime Institute of Technology) for 1 h at room temperature. After rinsing for 5 min three times with PBS, cell nuclei were counterstained with DAPI (0.2 µg/ml) for 10 min at 25°C, examined using CLSM and images were acquired.

Statistical analysis. Values are expressed as the mean \pm standard deviation and all data were evaluated separately from at least three independent experiments. Statistical comparisons were analyzed using GraphPad 5 (GraphPad Software Inc.). Statistical analysis was performed by application of Student's unpaired t-test and one-way ANOVA followed by Tukey's post-hoc test. P<0.05 was considered to indicate a statistically significant difference.

Results

Particle size and zeta potential of DTX/GA-HA-NPs. First, the physicochemical properties of the NPs were determined. The mean diameter, zeta potential and size distribution of DTX/GA-HA-NPs in the aqueous medium were measured using a laser particle analyzer and the results are provided in Table I and Fig. 1A and B. DTX/GA-HA-NPs had a negative zeta potential (-27.83 mV), which is caused by ionization of the carboxyl groups of HA and had favorable dispersibility in water [particle dispersity index (PDI), 0.21].

Morphological characterization. The morphological characterization of DTX/GA-HA-NPs was performed by TEM and an electron photomicrograph is provided in Fig. 2. The results indicated that DTX/GA-HA-NPs possessed an almost spherical shape and exhibited a relatively monodisperse distribution. The average NP diameter, as estimated from the TEM

Table I. Physicochemical property of DTX/GA-HA-NPs.

Sample	DLS, nm	PDI	SEM, nm	Zeta potential, mV	EE, %	LC, %
DTX/GA-HA-NPs	208.73±5.00	0.21±0.12	64.3±10.6	-27.83±3.14	85.38±4.62	17.59±0.68

Values are expressed as the mean ± standard deviation (n=3). PDI, particle dispersity index; DLS, Dynamic light scattering; LC, loading capacity; EE, encapsulation efficiency; DTX/GA-HA-NPs, docetaxel-loaded glycyrrhetic acid-modified hyaluronic acid nanoparticles.

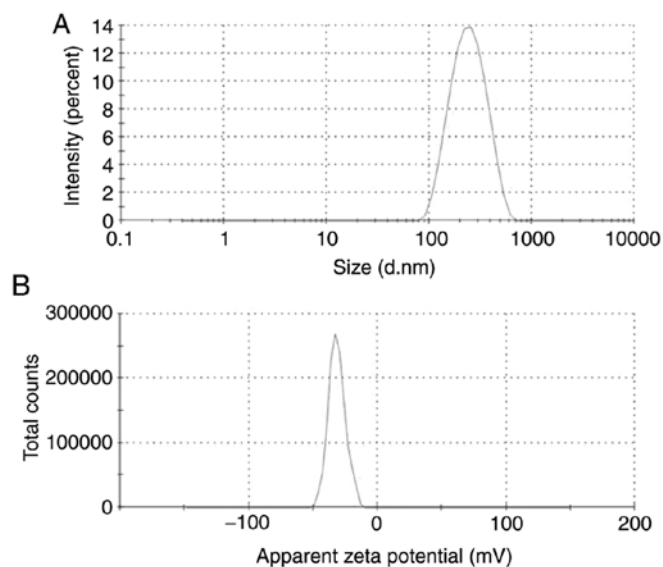


Figure 1. (A) Size distribution and (B) zeta potential of docetaxel-loaded glycyrrhetic acid-modified hyaluronic acid nanoparticles.

micrographs, was shown in Table I. This is smaller than the hydrodynamic diameter measured by the laser particle size analyzer.

Drug EE and LC. The EE and LC of DTX in DTX/GA-HA-NPs were measured by a simple dialysis method and by HPLC. A representative chromatogram of DTX is depicted in Fig. 3A. The results indicated that DTX had a retention time of 8.43 min. The standard curve for DTX exhibited linearity over the range of 10-80 $\mu\text{g/ml}$ (the concentration of standards are 10, 20, 40, 60 and 80 $\mu\text{g/ml}$) with a regression equation of $y=19.794x-1.023$ (Fig. 3B). The regression coefficient (R_2) for DTX over the specified range was calculated to be $R_2=0.9999$. According to the standard curve, the EE and LC of DTX were determined to be 85.38 ± 4.62 and $17.59\pm0.68\%$, respectively, as indicated in Table I.

Drug release profile. The DTX/GA-HA-NPs exhibited an initial fast release within 12 h, which may be attributed to the drug adhering to the NP surface. Within 12 to 24 h, DTX was also released slowly and the cumulative release amount reached an approximate maximum value (40%) at 24 h (Fig. 3C).

GA-HA-NPs have liver-targeting ability. A cell uptake study was performed for the qualitative estimation of the targeting ability of GA-HA-NPs and CLSM was used to observe the cellular localization of the GA-HA-NPs. To demonstrate the

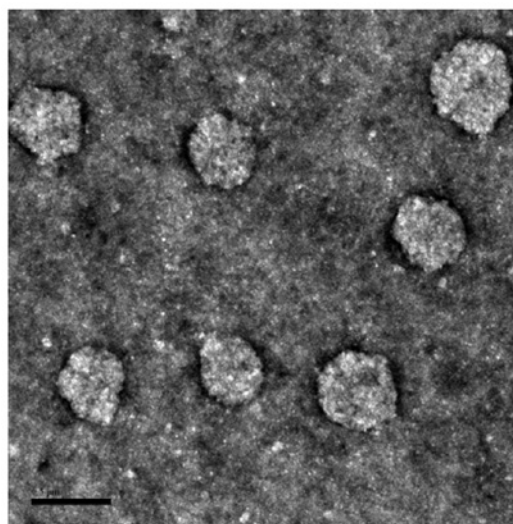


Figure 2. Transmission electron microscopy images of docetaxel-loaded glycyrrhetic acid-modified hyaluronic acid nanoparticles. Scale bar, 5 μm .

effect of GA-HA-NP targeting, receptor-mediated cellular uptake of FITC-GA-HA-NPs was studied in HepG2 cells and MCF-7 cells [negative for GA receptor (GA-R) expression] (36). Fluorescence images of the cells taken after 2 h of incubation with FITC-GA-HA-NPs are provided in Fig. 4A and B. The green fluorescence intensity was stronger in HepG2 than in MCF-7 cells.

HepG2 cells are more sensitive to DTX/GA-HA-NPs than free DTX. The CCK-8 assay is frequently used to detect the toxic effects of drugs on cells. It was thus used to evaluate the cytotoxic effects of free DTX and DTX/GA-HA-NPs on HepG2 cells. IC_{50} is the dose which led to a 50% reduction in viable cells compared with the control, reflecting the sensitivity of cells to drugs. The IC_{50} values of free DTX and DTX/GA-HA-NP after 24 h were 15.7 and 4.3 $\mu\text{g/ml}$ (equivalent free DTX), respectively (Table II), and the IC_{50} of DTX was 3.6 times that of DTX/GA-HA-NPs. After 48 h of incubation, the IC_{50} values of the free DTX and DTX/GA-HA-NPs cells were 3.8 and 1.6 $\mu\text{g/ml}$ (equivalent free DTX), respectively. Cell survival was lower with DTX/GA-HA-NPs compared with DTX as presented in Fig. 5. Therefore, HepG2 cells are more sensitive to DTX/GA-HA-NPs than free DTX.

DTX/GA-HA-NPs inhibit the colony formation ability of HepG2-cell. The effects of free DTX and DTX/GA-HA-NPs on the colony formation ability of HepG2 cells were also evaluated. Cells were incubated with an equivalent dose of

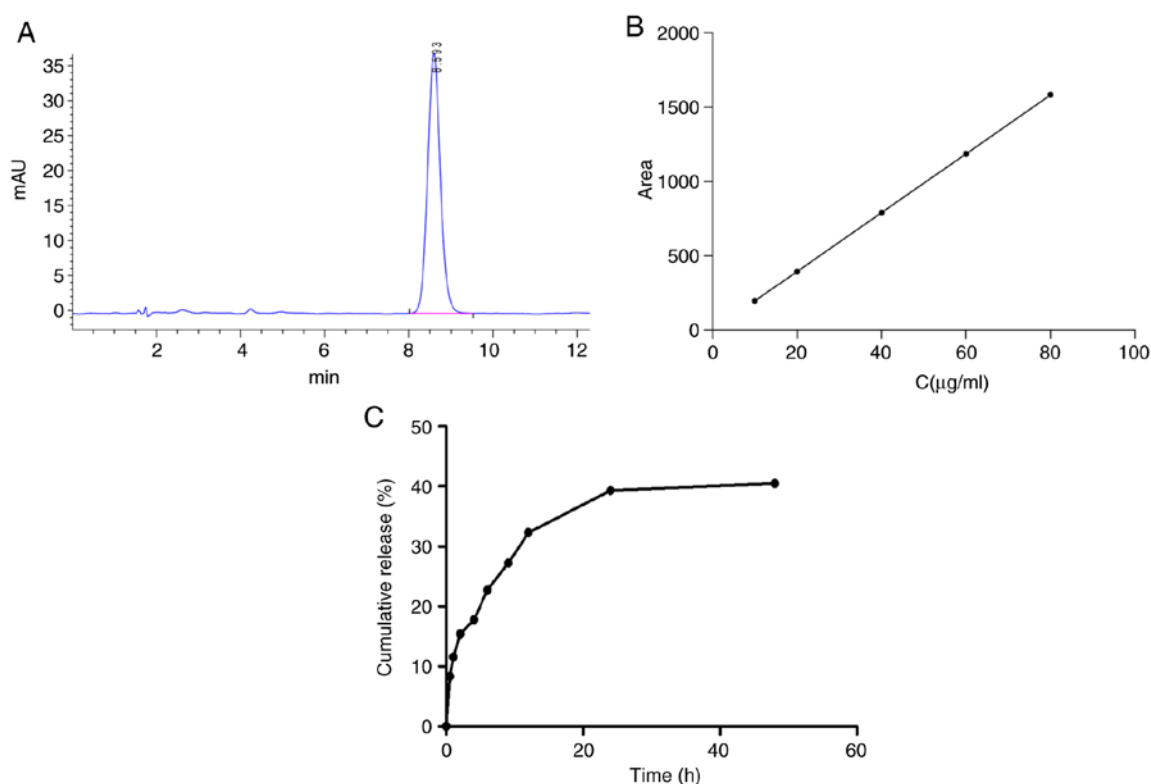


Figure 3. (A) High-performance liquid chromatogram of DTX with detection at 232 nm. (B) Calibration curve of DTX using linear regression model. (C) *In vitro* cumulative release profile of DTX from DTX-loaded glycyrrhetic acid-modified hyaluronic acid nanoparticles. DTX, docetaxel; C, concentration.

Table II. IC₅₀ values of DTX and DTX/GA-HA-NPs on HepG2 cells following 24 and 48 h of incubation, respectively.

Time (h)	IC ₅₀ , µg/ml	
	DTX	DTX/GA-HA-NPs
24	15.7±0.81	4.3±0.29
48	3.8±0.20	1.6±0.23

Values are expressed as the mean ± standard deviation (n=3). DTX/GA-HA-NPs, DTX-loaded glycyrrhetic acid-modified hyaluronic acid nanoparticles; DTX, docetaxel.

free DTX or DTX/GA-HA-NPs. As presented in Fig. 6, free DTX and DTX/GA-HA-NPs inhibited the colony formation of HepG2 cells in a dose- and time-dependent manner. However, the colony formation of HepG2 cells treated with DTX/GA-HA-NPs was significantly lower than that of cells treated with free DTX. In addition, a colony formation assay was performed to examine the antitumor effects of DTX/GA-HA-NPs against HepG2 cells. The number of colonies of HepG2 cells treated with DTX/GA-HA-NPs was significantly lower than that of control cells and cells treated with free DTX (Fig. 6). These results suggested that DTX/GA-HA-NPs significantly inhibited the colony formation ability of HepG2 cells.

DTX/GA-HA-NPs induce apoptosis of HepG2 cells. Fluorescence micrographs indicated that the morphology of

cells treated with DTX/GA-HA-NPs changed, and in certain cases, the nucleus was crescent-shaped or even broken (Fig. 7). Therefore, the percentage of apoptotic cells was measured using flow cytometry to assess whether DTX/GA-HA-NPs induced apoptosis in HepG2 cells. The results indicated that DTX/GA-HA-NPs significantly increased the percentage of apoptotic HepG2 cells (Fig. 8). It was thus indicated that DTX/GA-HA-NPs induce apoptosis in HepG2 cells.

DTX/GA-HA-NPs cause α -tubulin polymerization. According to previous studies, DTX binds to the α -tubulin subunit of microtubulin to cause tubulin polymerization. Immunofluorescence staining technology was utilized to examine the effects of DTX/GA-HA-NPs on HepG2 microtubule cytoskeletons. As presented in Fig. 9, red fluorescent staining of tubulin in untreated cells indicated intact cell morphology and generally cytoplasmic distribution, while staining of cells treated with DTX revealed partial polymerization and a slight change in cell morphology. By contrast, cells treated with DTX/GA-HA-NPs exhibited a large degree of tubulin polymerization around their nuclei, less tubulin in the cytoplasm and a markedly distorted morphology.

Discussion

NPs are nano-scale solid colloidal particles made of natural or synthetic polymer carrier materials. As a drug delivery carrier, NPs have unique advantages such as low toxicity, controlled release, good stability and strong targeting. NPs have unique advantages and potential application value in the field of NP-targeted drug delivery systems. Ligand-functionalized

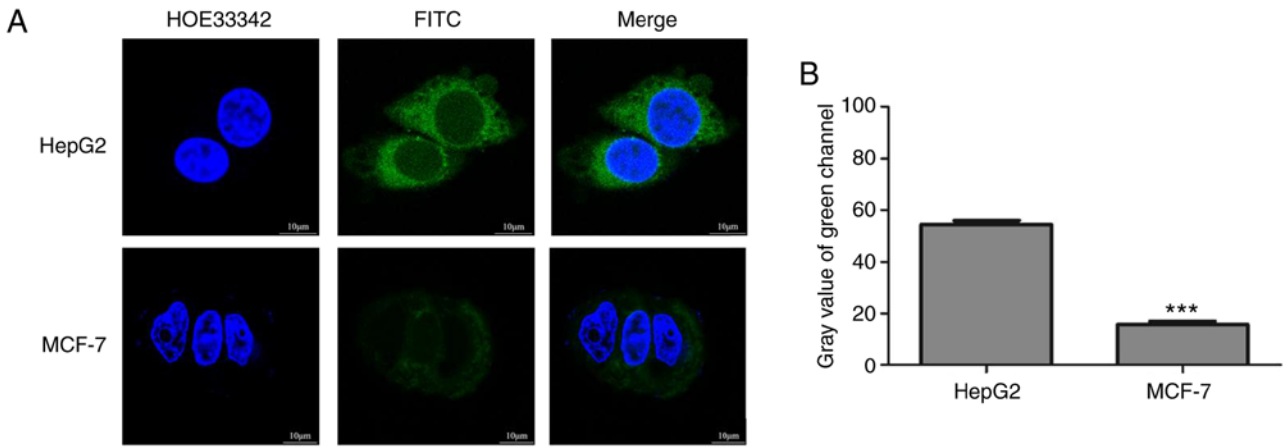


Figure 4. GA-HA-NPs have cell-targeting ability. (A) Confocal laser scanning microscopy images of different cells after 2 h of FITC/GA-HA-NP treatment. All samples had an FITC/GA-HA concentration of 600 μg/ml (scale bar, 10 μm). (B) Cellular uptake efficiency of FITC/GA-HA by different cells after 2 h. *** $P < 0.001$. GA-HA-NPs, glycyrrhetic acid-modified hyaluronic acid nanoparticles; HOE, Hoechst.

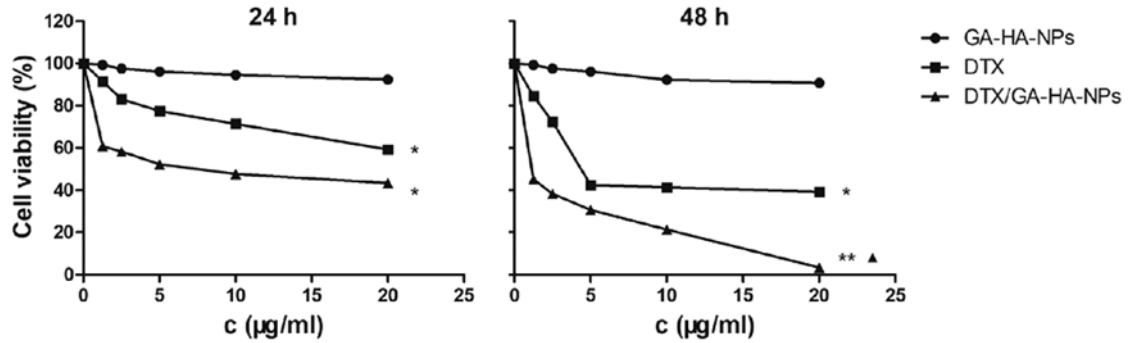


Figure 5. Proliferative effects of GA-HA-NPs, DTX and DTX/GA-HA-NPs on HepG2 cells. * $P < 0.05$, ** $P < 0.01$ vs. GA-HA-NP group; # $P < 0.05$ vs. DTX group. DTX, docetaxel; DTX/GA-HA-NPs, DTX-loaded GA-HA nanoparticles; GA-HA, glycyrrhetic acid-modified hyaluronic acid.

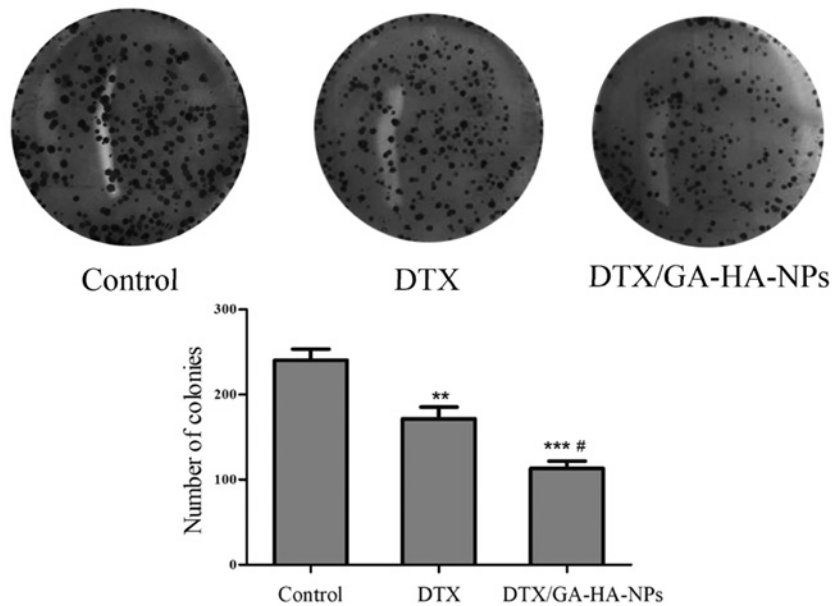


Figure 6. Effects of DTX/GA-HA-NPs on the colony formation ability of HepG2 cells. ** $P < 0.01$, *** $P < 0.001$ vs. control group; # $P < 0.05$ vs. DTX group. DTX, docetaxel; DTX/GA-HA-NPs, DTX-loaded GA-HA nanoparticles; GA-HA, glycyrrhetic acid-modified hyaluronic acid.

NPs are able to deliver drugs to targets. The preparation materials of NPs include natural polymer materials, synthetic

polymer materials and non-degradable polymer materials. Zhang *et al* (37) coupled HA with aminated GA and prepared

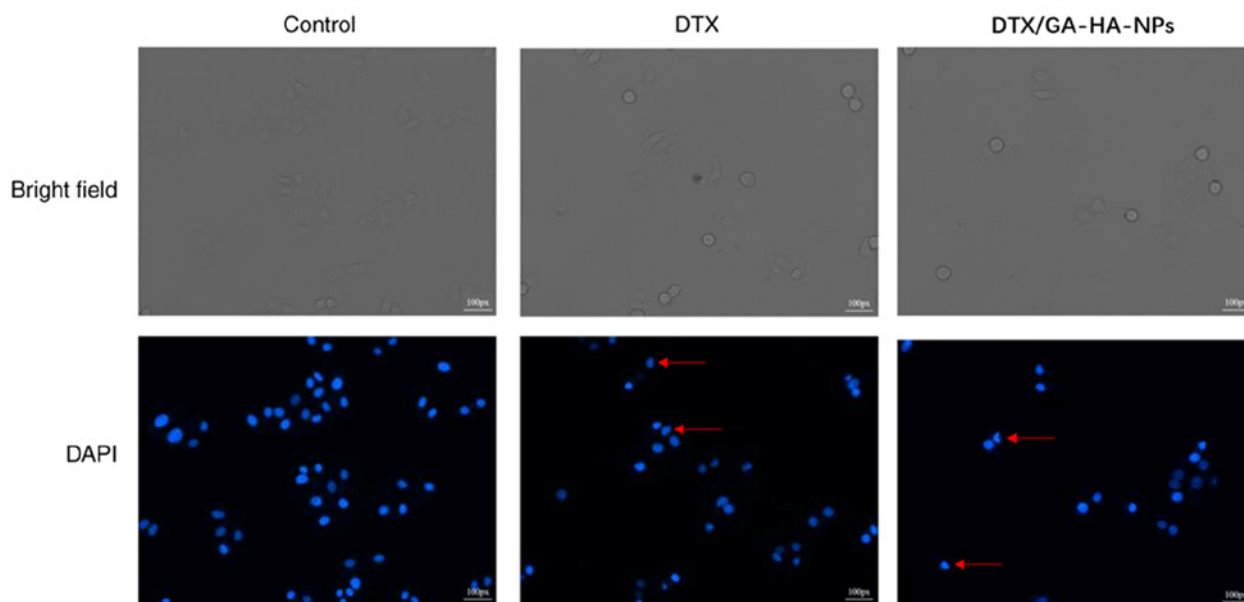


Figure 7. Effects of DTX and DTX/GA-HA-NPs on HepG2 cell apoptosis according to DAPI staining. Morphological changes of the nucleus was recorded after the treatments of different drugs and a deformed nucleus and formation of apoptotic bodies were observed. DTX, docetaxel; DTX/GA-HA-NPs, DTX-loaded GA-HA nanoparticles; GA-HA, glycyrrhetic acid-modified hyaluronic acid. Scale bar, 100 pixels, 8,500 μm)

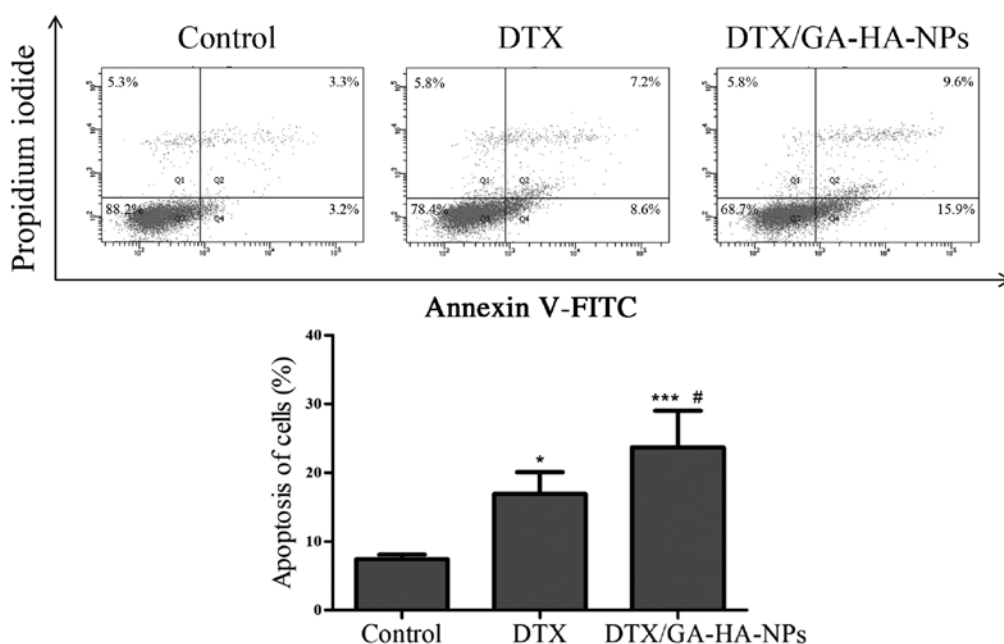


Figure 8. Flow cytometric analysis of apoptosis induced by DTX and DTX/GA-HA-NPs. * $P < 0.05$, *** $P < 0.001$ vs. control group; # $P < 0.05$ vs. DTX group. DTX, docetaxel; DTX/GA-HA-NPs, DTX-loaded GA-HA nanoparticles; GA-HA, glycyrrhetic acid-modified hyaluronic acid.

GA-HA-NPs as a carrier to deliver PTX. Their results indicated that GA-HA-NPs easily encapsulate PTX, with drug LC and EE of as high as 31.16 and 92.02%, respectively, and the cytotoxicity of HepG2 cells was greater than that of B16F10 cells.

In the present study, DTX/GA-HA-NPs were indicated to have a smaller particle size compared to GA/HA-NPs. This smaller particle size may be due to the hydrophobicity of the DTX encapsulated in the GA-HA-NPs. Hydrophobic interactions between the component materials give the DTX/GA-HA-NPs a more compact core. Furthermore, the

particle size of DTX/GA-HA-NPs measured by TEM was smaller than that obtained with the particle size analyzer. This difference may be due to different sample preparation techniques; the laser particle analyzer measurements were made under aqueous conditions, while the TEM images were obtained with dried samples in which the hydrophilic shells of the DTX/GA-HA-NPs may have shrunk.

During the preparation of GA-HA and DTX/GA-HA, the excess organic solvent was removed by dialysis. Dialysis is a purification technique used to prepare biomacromolecules, featuring desalination, removal of small amounts of organic

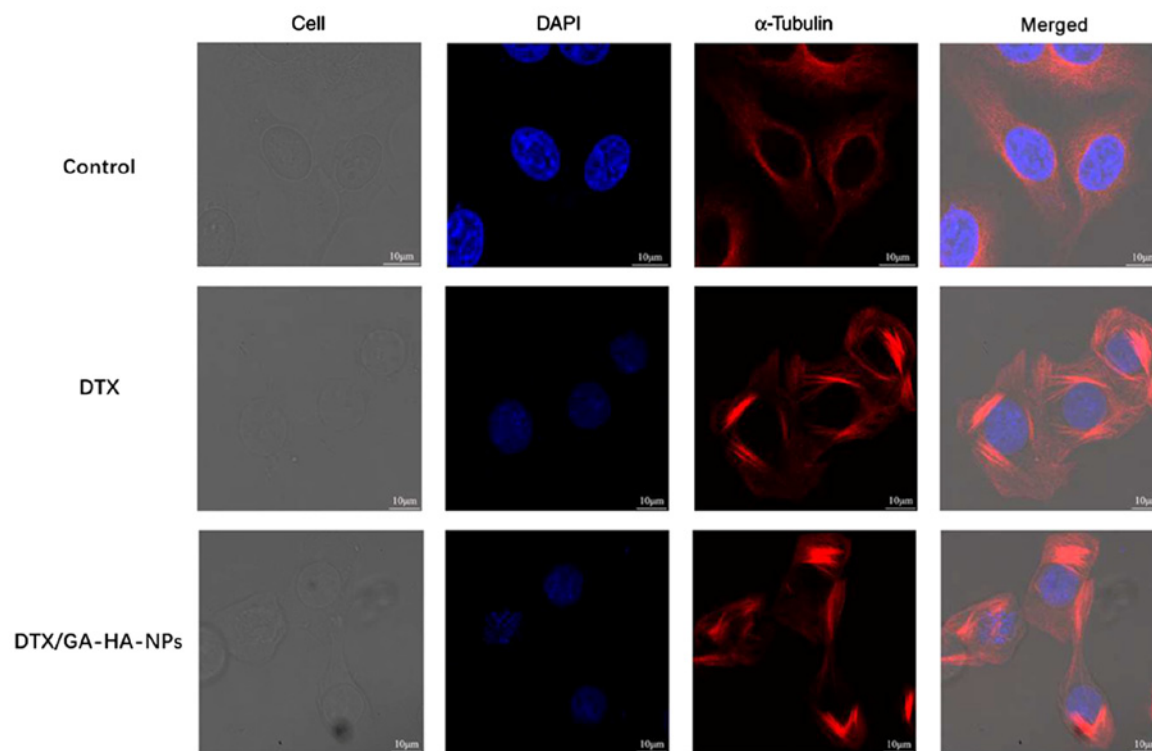


Figure 9. Effects of DTX/GA-HA on the microtubule cytoskeleton of HepG2 cells (scale bar, 10 μm). DTX, docetaxel; DTX/GA-HA-NPs, DTX-loaded GA-HA nanoparticles; GA-HA, glycyrrhetic acid-modified hyaluronic acid.

solvents, removal of small biomolecule impurities and sample concentration. The dialysis method is able to separate the excess materials, drugs and related solvents (such as formamide, ethanol) used during the synthesis of DTX/GA-HA-NPs from the product and thus purify DTX/GA-HA-NPs. Therefore, dialysis was used to remove excess drug, materials and related solvents.

DTX enters cells through passive diffusion. In the DTX/GA-HA-NPs prepared in the present study, GA has a role in liver targeting and GA-R-mediated endocytosis may be a key mechanism by which DTX/GA-HA-NPs target the liver (38). Using GA-modified NPs as a carrier of liver-targeted drugs provides a novel solution for the treatment of liver cancer. Studies have indicated that, whether it is the introduction of GA molecules on the C30-carboxyl group or the C3-hydroxyl group, GA-modified NPs have the same tendency to target the liver. The most common modification is the amidation and esterification of GA and C30-carboxy to obtain more active compounds, this was also the method used in the present study. In the modified C3-hydroxyl group of GA, the C30-carboxyl group should be protected first because of its high activity and then the C3-hydroxyl group should be amidated and esterified.

To examine the uptake and intracellular localization of FITC-loaded GA-HA-NPs, two cell lines were selected for comparison. The results indicated that the fluorescence of FITC-GA-HA in HepG2 was stronger than that in MCF-7 cells. Among these cells, GA-R is widely expressed on human liver cancer HepG2 cells (33,34). Therefore, GA receptor-mediated endocytosis may be a key mechanism by which GA-HA-NPs target the liver. In 1990, Aruffo *et al* (39) reported that CD44 is the major cell surface receptor of HA

and that HA is able to actively target the surfaces of liver cancer cells to bind to the CD44 receptor and be taken up by endocytosis. Zhang *et al* (37) coupled HA with aminated GA and prepared GA-HA-NPs as carriers to deliver PTX. Confocal microscopy indicated that the *in vitro* cellular uptake of FITC-labeled GA-HA-NPs was higher than that of free FITC and the green fluorescence intensity of HepG2 cells and B16F10 cells was higher than that of HELF cells (normal fibroblasts), indicating that the mechanism of GA-HA targeting may be the interaction between HA and the CD44 receptor. Therefore, the breast cancer cell line MCF-7 with no GA receptors expressed was selected for an uptake study and a relatively smaller amount of fluorescence was observed in the cytoplasm. Uptake by MCF-7 cells may have been due to the binding affinity of HA to the CD44 receptor. Therefore, HepG2 cells were used for subsequent studies. In a preliminary experiment for the present study, GA was added in advance and incubation was performed for 2 h, followed by the addition of DTX/GA-HA, and it was indicated that the fluorescence intensity was decreased compared with the one with no GA incubation, suggesting that during the pre-incubation, GA combined with the GA-R on the surface of liver cancer cells, competitively inhibiting the binding of DTX/GA-HA to GA-R, thereby inhibiting the uptake of DTX/GA-HA (data not shown).

A mechanism for the cellular uptake of DTX/GA-HA and release of DTX in cancer cells was proposed and illustrated in a schematic in Fig. 10. GA and HA self-aggregate to form GA-HA, which is packaged with DTX to form DTX/GA-HA-NPs. GA directs NPs to the surface of liver/liver cancer cells, binds to GA-R receptors, enters cells through endocytosis and exocytosis and releases DTX

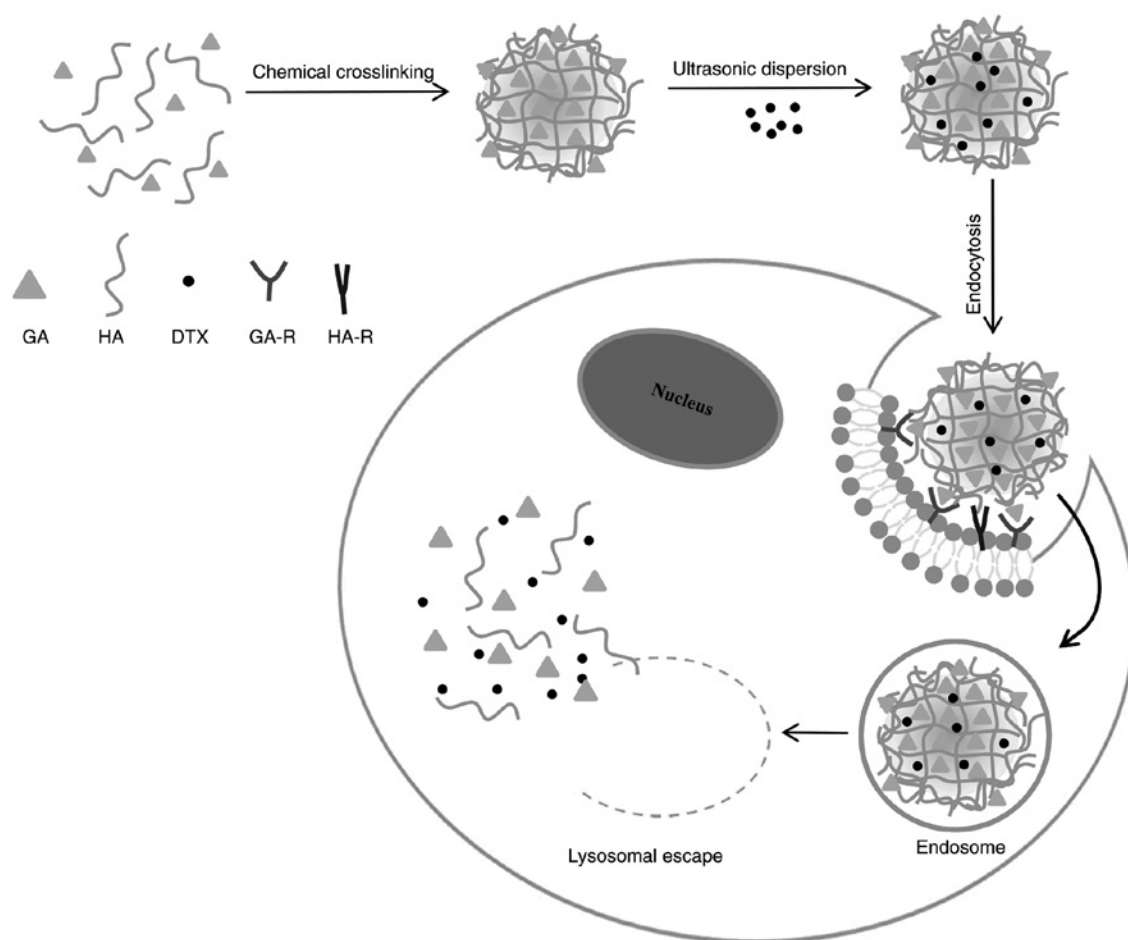


Figure 10. Schematic of DTX/GA-HA-NPs and release of DTX inside cancer cells. DTX, docetaxel; GA, glycyrrheticin; HA, hyaluronic acid; DTX/GA-HA-NPs, DTX-loaded GA-modified HA nanoparticles; R, receptor.

through lysosome to exert its efficacy (Fig. 10). However, the process by which FITC-GA-HA is taken up by cells and the associated biochemical events warrant further study.

All drugs known to bind human tubulin are associated with β -tubulin, including DTX. Previous studies have confirmed that DTX binds the β -tubulin unit, resulting in tubulin polymerization (40,41). Therefore, α -tubulin was chosen for verification and it was determined that DTX is also able to enhance the polymerization of cellular tubulin by binding α -tubulin. Therefore, the polymerization of DTX on the cellular microtubule system is able to halt the cell cycle by preventing mitosis. It was hypothesized that DTX and DTX/GA-HA-NPs act on microtubules, affecting spindle formation and causing cells to lose their dividing dynamics, thereby inhibiting cell proliferation. Wang *et al* (42) concluded that this blocking of the mitotic phase is the cause of taxane-induced cytotoxicity. However, the biochemical events associated with taxanes binding to microtubules and downstream effects to cause apoptosis remain to be fully elucidated. Further research by our group will aim to verify the effects of DTX on cell cycle regulation to confirm its mechanism of action.

In the present study, the ability of DTX to inhibit tumor cell proliferation was examined. Inhibitory effects on proliferation were examined by CCK-8 and cell colony formation assays. It was first observed that the viability of HepG2 cells

treated with empty GA-HA-NPs was >90%, which was consistent with previous studies (35) and indicated the biosafety of the nanocarriers. The calculated IC_{50} values indicated that HepG2 cells were more sensitive to DTX/GA-HA-NPs than free DTX. Furthermore, the CCK-8 assay indicated that the viability of HepG2 cells significantly decreased after incubation with DTX and DTX/GA-HA-NPs. After 24 h, the cell viability was <60% compared with the control. After 48 h, the cell viability in the DTX group was <40%, while cell viability in the DTX/GA-HA-NP group was <10% compared with the control group. Thus, docetaxel effectively inhibits HepG2 cell proliferation and this effect was enhanced by the delivery of the drug via DTX/GA-HA-NPs. Similarly, it was further confirmed by cell colony formation assay that DTX/GA-HA-NPS can significantly inhibit the growth of HepG2 cells.

Wang *et al* (42) observed multiple roles of microtubules in cell cycle and apoptosis regulation. In the present study, it was observed that treatment with DTX and DTX/GA-HA-NPs induced nuclear contraction and deformation in the cells stained with DAPI. In addition, flow cytometric analysis was performed and it was determined that the apoptotic rate of HepG2 cells after incubation with DTX and DTX/GA-HA-NPs was 18 and 24%, respectively. The result of the present study was consistent with a previous study (43), which also indicated DTX/GA-HA-NPs had

higher delivery efficacy to liver cancer cells compare to free drugs.

The present study only verified the liver targeting and anti-tumor effects of DTX/GA-HA at the cellular level and did not study the metabolism and kinetic effects of the drug *in vivo*. Next, tumor-bearing experiments and *in vivo* small animal imaging experiments will be performed by our group to study the liver targeting and anti-tumor activity of DTX/GA-HA *in vivo*.

In summary, DTX/GA-HA was successfully prepared, which had good physical and chemical properties. Furthermore, it had a good liver cancer cell targeting effect *in vitro*, but the GA-mediated liver targeting transmembrane mechanism requires further research. Subsequent to the study of its *in vitro* anti-cancer activity, it is necessary to clarify the role of DTX/GA-HA in inhibiting tumor activity and how it affects the cell cycle, which may provide a good foundation for further research on its anti-tumor effect *in vivo*.

Acknowledgements

Not applicable.

Funding

This work was supported by grants from the National Natural Science Foundation of China (grant nos. 81274093 and 81871892) and the Natural Science Foundation of Shandong Province (grant no. ZR2019MC042).

Availability of data and materials

The datasets used and/or analyzed during the current study are available from the corresponding author on reasonable request.

Authors' contributions

ZG, YW and HX were responsible for the conception of this work. FW, BL and HX performed the preliminary synthesis of GA-HA and DTX/GA-HA-NPs. TS, XL, CW and LZ performed the characterization of NPs. WD, JB, CZ and LQ contributed to cell experiments (including cell culture, cell proliferation experiments, clonogenicity experiments and apoptosis experiments). HX, BJ, MQ and WW performed experiments on the microtubule aggregation effect of DTX/GA-HA and HX was a major contributor in writing the manuscript. JW and WY assisted with the data analysis and drafted the discussion part of the manuscript. YW and ZG confirmed the authenticity of all the raw data and approved the final manuscript. All authors read and approved the final manuscript.

Ethics approval and consent to participate

Not applicable.

Patient consent for publication

Not applicable.

Competing interests

The authors declare that they have no competing interests.

References

- Natarajan Y, Kramer JR, Yu X, Li L, Thrift AP, El-Serag HB and Kanwal F: risk of cirrhosis and hepatocellular cancer in patients with non-alcoholic fatty liver disease and normal liver enzymes. *Hepatology* 72: 1242-1252, 2020.
- Sagnelli E, Macera M, Russo A, Coppola N and Sagnelli C: Epidemiological and etiological variations in hepatocellular carcinoma. *Infection* 48: 7-17, 2020.
- Dimitroulis D, Damaskos C, Valsami S, Davakis S, Garmpis N, Spartalis E, Athanasiou A, Moris D, Sakellariou S, Kykalos S, *et al*: From diagnosis to treatment of hepatocellular carcinoma: An epidemic problem for both developed and developing world. *World J Gastroenterol* 23: 5282-5294, 2017.
- Sun W, Wang Y, Cai M, Lin L, Chen X, Cao Z, Zhu K and Shuai X: Codelivery of sorafenib and GPC3 siRNA with PEI-modified liposomes for hepatoma therapy. *Biomater Sci* 5: 2468-2479, 2017.
- Lu B, Yu GJ and Cheng M: Expression and clinical significance of Snail and Claudin-3 in primary hepatocellular carcinoma. *Shandong Yiyao* 58: 6-9, 2018 (In Chinese).
- Zhang H, Wu Y, Hu Y, Li X, Zhao M and Lv Z: Targeted nanoparticle drug delivery system for the enhancement of cancer immunotherapy. *J Biomed Nanotechnol* 15: 1839-1866, 2019.
- Wu Y, Xu Z, Sun W, Yang Y, Jin H, Qiu L, Chen J and Chen J: Co-responsive smart cyclodextrin-gated mesoporous silica nanoparticles with ligand-receptor engagement for anti-cancer treatment. *Mater Sci Eng C* 103: 109831, 2019.
- Lin A, Chen J, Liu Y, Deng S, Wu Z, Huang Y and Ping Q: Preparation and evaluation of N-caproyl chitosan nanoparticles surface modified with glycyrrhizin for hepatocyte targeting. *Drug Dev Ind Pharm* 35: 1348-1355, 2009.
- Sun Y, Dai C, Yin M, Lu J, Hu H, Chen D: Hepatocellular carcinoma-targeted effect of configurations and groups of glycyrrhetic acid by evaluation of its derivative-modified liposomes. *Int J Nanomedicine* 13: 1621-1632, 2018.
- Yan T, Cheng J, Liu Z, Cheng F, Wei X, Huang Y and He J: Acid-sensitive polymeric vector targeting to hepatocarcinoma cells via glycyrrhetic acid receptor-mediated endocytosis. *Mater Sci Eng C* 87: 32-40, 2018.
- Sakurai Y and Harashima H: Hyaluronan-modified nanoparticles for tumor-targeting. *Expert Opin Drug Deliv* 16: 915-936, 2019.
- Tavianatou AG, Caon I, Franchi M, Piperigkou Z, Galesso D and Karamanos NK: Hyaluronan: Molecular size-dependent signaling and biological functions in inflammation and cancer. *FEBS J* 286: 2883-2908, 2019.
- Tirella A, Kloc-Muniak K, Good L, Ridden J, Ashford M, Puri S and Tirelli N: CD44 targeted delivery of siRNA by using HA-decorated nanotechnologies for KRAS silencing in cancer treatment. *Int J Pharm* 561: 114-123, 2019.
- Li W, Yan R, Liu Y, He C, Zhang X, Lu Y, Khan MW, Xu C, Yang T and Xiang G: Co-delivery of Bmi1 small interfering RNA with ursolic acid by folate receptor-targeted cationic liposomes enhances anti-tumor activity of ursolic acid in vitro and in vivo. *Drug Deliv* 26: 794-802, 2019.
- Yu Y, Wang J, Kaul SC, Wadhwa R and Miyako E: Folic acid receptor-mediated targeting enhances the cytotoxicity, efficacy, and selectivity of withania somnifera leaf extract: In vitro and in vivo evidence. *Front Oncol* 9: 602, 2019.
- Cai Y, Xu Y, Chan HF, Fang X, He C and Chen M: Glycyrrhetic acid mediated drug delivery carriers for hepatocellular carcinoma therapy. *Mol Pharm* 13: 699-709, 2016.
- He ZY, Zheng X, Wu XH, Song XR, He G, Wu WF, Yu S, Mao SJ and Wei YQ: Development of glycyrrhetic acid-modified stealth cationic liposomes for gene delivery. *Int J Pharm* 397: 147-154, 2010.
- Gao S, Wang J, Tian R, Wang G, Zhang L, Li Y, Li L, Ma Q and Zhu L: Construction and evaluation of a targeted hyaluronin acid nanoparticle/photosensitizer complex for cancer photodynamic therapy. *ACS Appl Mater Interfaces* 9: 32509-32519, 2017.
- Fang Z, Li X, Xu Z, Du F, Wang W, Shi R and Gao D: Hyaluronin acid-modified mesoporous silica-coated superparamagnetic Fe₃O₄ nanoparticles for targeted drug delivery. *Int J Nanomedicine* 14: 5785-5797, 2019.

20. Tian G, Sun X, Bai J, Dong J, Zhang B, Gao Z and Wu J: Doxorubicin loaded dual functional hyaluronic acid nanoparticles: Preparation, characterization and antitumor efficacy in vitro and in vivo. *Mol Med Rep* 19: 133-142, 2019.
21. Duan T, Xu Z, Sun F, Wang Y, Zhang J, Luo C and Wang M: HPA aptamer functionalized paclitaxel-loaded PLGA nanoparticles for enhanced anticancer therapy through targeted effects and microenvironment modulation. *Biomed Pharmacother* 117: 109121, 2019.
22. Handali S, Moghimipour E, Kouchak M, Ramezani Z, Amini M, Angali KA, Saremy S, Dorkoosh FA and Rezaei M: New folate receptor targeted nano liposomes for delivery of 5-fluorouracil to cancer cells: Strong implication for enhanced potency and safety. *Life Sci* 227: 39-50, 2019.
23. Patel NR, Piroyan A, Ganta S, Morse AB, Candiloro KM, Solon AL, Nack AH, Galati CA, Bora C, Maglaty MA, *et al*: In vitro and in vivo evaluation of a novel folate-targeted theranostic nanoemulsion of docetaxel for imaging and improved anticancer activity against ovarian cancers. *Cancer Biol Ther* 19: 554-564, 2018.
24. Ren J, Chen Y, Song H, Chen L and Wang R: Inhibition of ZEB1 reverses EMT and chemoresistance in docetaxel-resistant human lung adenocarcinoma cell line. *J Cell Biochem* 114: 1395-1403, 2013.
25. Cortes JE and Pazdur R: Docetaxel. *J Clin Oncol* 13: 2643-2655, 1995.
26. Taxanes. In: *LiverTox: Clinical and Research Information on Drug-Induced Liver Injury*, 2020.
27. Belderbos BP, Hussaarts KG, van Harten LJ, Oomen-de Hoop E, de Bruijn P, Hamberg P, van Alphen RJ, Haberkorn BC, Lolkema MP, de Wit R, *et al*: Effects of prednisone on docetaxel pharmacokinetics in men with metastatic prostate cancer: A randomized drug-drug interaction study. *Br J Clin Pharmacol* 85: 986-992, 2019.
28. Wu F, Zhang LX, Li XC, Jiang B, Zou SY, Wang C, Mou WQ, Lian B, Wu JL, Yu WJ, *et al*: Preparation and proliferation effect on hepatoma cells of adenine loaded glycyrrhetic acid modified hyaluronic acid nanoparticles. *Zhongguo Yaolixue Tongbao* 34: 706-712, 2018 (In Chinese).
29. Kothari IR, Italiya KS, Sharma S, Mittal A and Chitkara D: A rapid and precise liquid chromatographic method for simultaneous determination of alpha lipoic acid and docetaxel in lipid-based nanoformulations. *J Chromatogr Sci* 56: 888-894, 2018.
30. Lou YM and Huang ZB: Determination of the related substances in docetaxel for drug materials by HPLC. *Pharm J* 23: 41-44, 2011.
31. Cha L, Gu YH and Wang YL: Determination of docetaxel drug substance by HPLC. *J Hubei Univ Sci Technol* 31: 3-5, 2017.
32. Stanković V, Mihailović V, Mitrović S and Jurišić V: Protective and therapeutic possibility of medical herbs for liver cirrhosis. *Rom J Morphol Embryol* 58: 723-729, 2017.
33. Li X, Diao W, Xue H, Wu F, Wang W, Jiang B, Bai J, Lian B, Feng W, Sun T, *et al*: Improved efficacy of doxorubicin delivery by a novel dual-ligand-modified liposome in hepatocellular carcinoma. *Cancer Lett* 489: 163-173, 2020.
34. Li ZP, Tian GX, Jiang H, Pan RY, Lian B, Wang M, Gao ZQ, Zhang B, Wu JL, *et al*: Liver-targeting and pH-sensitive sulfated hyaluronic acid mixed micelles for hepatoma therapy. *Int J Nanomedicine* 14: 9437-9452, 2019.
35. Jurisic V, Srdic-Rajic T, Konjevic G, Bogdanovic G and Colic M: TNF- α induced apoptosis is accompanied with rapid CD30 and slower CD45 shedding from K-562 cells. *J Membr Biol* 239: 115-122, 2011.
36. Wu F, Xue H, Li X, Diao W, Jiang B, Wang W, Yu W, Bai J, Wang Y, Lian B, *et al*: Enhanced targeted delivery of adenine to hepatocellular carcinoma using glycyrrhetic acid-functionalized nanoparticles in vivo and in vitro. *Biomed Pharmacother* 131: 110682, 2020.
37. Zhang L, Yao J, Zhou J, Wang T and Zhang Q: Glycyrrhetic acid-graft-hyaluronic acid conjugate as a carrier for synergistic targeted delivery of antitumor drugs. *Int J Pharm* 441: 654-664, 2013.
38. Wu F, Li X, Jiang B, Yan J, Zhang Z, Qin J, Yu W and Gao Z: Glycyrrhetic acid functionalized nanoparticles for drug delivery to liver cancer. *J Biomed Nanotechnol* 14: 1837-1852, 2018.
39. Aruffo A, Stamenkovic I, Melnick M, Underhill CB and Seed B: CD44 is the principal cell surface receptor for hyaluronate. *Cell* 61: 1303-1313, 1990.
40. Xiao H and Wang L: Effects of X-shaped reduction-sensitive amphiphilic block copolymer on drug delivery. *Int J Nanomedicine* 10: 5309-5325, 2015.
41. Doddapaneni R, Patel K, Chowdhury N and Singh M: Noscapine chemosensitization enhances docetaxel anticancer activity and nanocarrier uptake in triple negative breast cancer. *Exp Cell Res* 346: 65-73, 2016.
42. Wang TH, Wang HS and Soong YK: Paclitaxel-induced cell death: Where the cell cycle and apoptosis come together. *Cancer* 88: 2619-2628, 2000.
43. Chen YN, Hsu SL, Liao MY, Liu YT, Lai CH, Chen JF, Nguyen MT, Su YH, Chen ST and Wu LC: Ameliorative effect of curcumin-encapsulated hyaluronic acid-PLA nanoparticles on thioacetamide-induced murine hepatic fibrosis. *Int J Environ Res Public Health* 14: 11, 2016.



This work is licensed under a Creative Commons Attribution-NonCommercial-NoDerivatives 4.0 International (CC BY-NC-ND 4.0) License.